Int. J. Heat Mass Transfer. Vol. 31, No. 5, pp. 931–940, 1988
Printed in Great Britain

0017–9310/88 $3.00 + 0.00

Steady-state analysis of two-phase natural circulation loop

K. S. CHEN† and Y. R. CHANG
Department of Mechanical Engineering, National Sun Yat-Sen University, Kaohsiung, Taiwan 800, Republic of China

(*Received* 10 *July* 1987 *and in final form* 14 *September* 1987)

Abstract—This paper is concerned with the steady-state behaviour of two-phase natural circulation loops, i.e. thermosyphon loops, in which the density difference of a fluid between its liquid and vapour phases is the driving force. The one-dimensional governing equations are first formulated for a variable-area, two-phase loop based on the homogeneous model. In addition, the quality of the vapour in the two-phase zone is assumed to be a linearly varying function of the flow distance. The model is then applied to constant-area square and toroidal loops with water–steam as the working fluid. For a given size and shape of the loop, the effect of relative position between the evaporator and condenser can be evaluated in terms of the water-level difference between them. Results show that loop mass flow rate and recovered heat increase with increasing water-level difference under a fixed two-phase zone length due to the increase of the buoyant force, while they decrease with increasing two-phase zone length under a fixed water-level difference due to the increase of the two-phase frictional force. For a given loop diameter or loop length, the mass flow rate and the recovered heat decrease with decreasing flow cross-sectional area under fixed water-level difference and two-phase zone length primarily due to the decrease of inertial force around the loop. For the purpose of waste heat recovery, a fluid with larger latent heat of evaporation is desirable since it is able to recover more heat for a given mass flow rate.

1. INTRODUCTION

THIS PAPER is concerned with the steady-state behaviour of a two-phase natural circulation loop, i.e. thermosyphon loop, in which the density difference of a fluid between its liquid and vapour phases is the driving force. There are a number of engineering applications for a two-phase natural circulation loop. Examples are thermosyphon reboilers [1–3], emergency cooling of nuclear reactor cores during an accident [4, 5] and reflux boiling in a light water reactor core [6]. Of equal importance in engineering applications is the single phase natural circulation loops, such as the cooling loop in a pressurized water reactor core, solar water heaters, and cooling of turbine blades and electronic components; see refs. [7–9].

Demands on energy conservation also put it into use for waste heat recovery. A recently commercialized unit for such a purpose is a two-phase rectangular loop shown in Fig. 1; see ref. [10]. There, a high-temperature flue gas is forced to pass through the evaporator section located at one vertical branch, while the preheated air is forced to pass through the condenser section located on another vertical branch of the loop, within which water–steam is circulating. For proper circulation in such a system, the evaporator section should be placed below the condenser. The vertical distance between the evaporator and condenser sections, their lengths and flow cross-sectional area are the main parameters that affect the loop performance.

Ramos *et al.* [11] carried out a one-dimensional steady-state analysis for two-phase loops and discussed the effect of water-level difference, i.e. the vertical distance between evaporator and condenser, on the loop mass flow rate. The analysis, however, is based on the 'sharp-interface' approximation in which two-phase zone lengths in the evaporator and condenser sections are neglected. In so doing, effects of two-phase zone lengths and more insight phenomena affecting the loop performance cannot be examined.

It is the purpose of this paper to provide a detailed steady-state, one-dimensional, analysis of natural circulation loops. The governing equations are first formulated for a variable-area, two-phase loop based on the homogeneous model. In addition, the quality of the vapour in the two-phase zone is assumed to be a linearly varying function of the flow distance. The model is then applied to constant-area square and toroidal loops with water–steam as the working fluid. Effects of water-level difference, two-phase zone lengths, and flow cross-sectional area on the loop mass flow rate and recovered heat are examined and discussed.

2. MATHEMATICAL FORMULATION FOR VARIABLE-AREA LOOP

The closed loop has an arbitrary shape with a prescribed cross-sectional area $A(s)$, where s is the coordinate measured from the origin in the counter-

† To whom all correspondence should be addressed.

NOMENCLATURE

A	flow cross-sectional area
B	proportional factor for the frictional force in a single phase zone
D	diameter of flow cross-sectional area
f_{TP}	two-phase friction coefficient
g	gravitational acceleration
h_{fg}	latent heat of vaporization
L	total length of the loop
l	length of two-phase zone when $l_h = l_c = l$
l_c	length of cooling (condenser) section
l_h	length of heating (evaporator) section
$\dot{m}$	mass flow rate
P	perimeter of flow cross-section
p	local pressure
$\dot{Q}$	total heat input (or output)
$\dot{q}_c$	heat output per unit length
$\dot{q}_h$	heat input per unit length
R	radius of toroidal loop (Fig. 4)
s	coordinate or flow distance
u	mean velocity
x	quality of vapour in two-phase zone
z	vertical height relative to a datum plane (Fig. 1).

Greek symbols

Δ	difference
θ	angle of flow direction from the horizontal for a square loop (Fig. 3); or angle measured from the lowest point in a toroidal loop (Fig. 4)
μ	dynamic viscosity
v	specific volume
v_{fg}	difference in specific volume between saturated vapour and its liquid
ρ	density
τ_w	frictional force on the wall.

Subscripts

c	cooling section in the loop
g	vapour or gas
h	heating section in the loop
l	liquid.

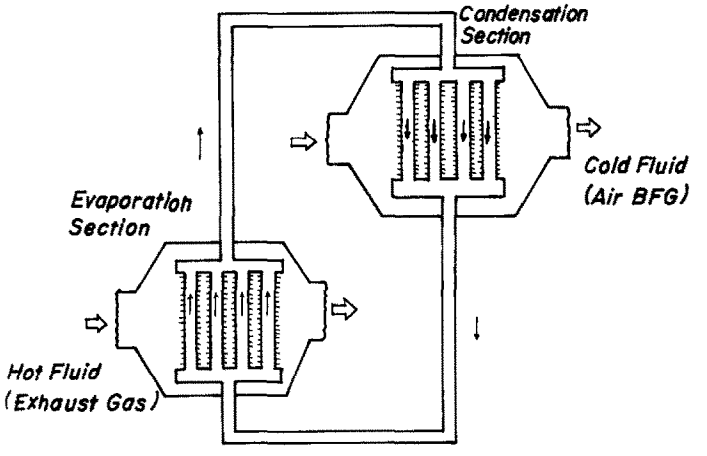

FIG. 1. Schematic of a two-phase natural circulation loop for waste heat recovery.

clockwise direction (Fig. 2). The section $0 < s \leqslant d_1$ is adiabatic and contains saturated liquid. The loop is heated continuously by a constant heat flux $\dot{q}_h$ in the evaporator region $d_1 < s \leqslant d_2$. Section $d_2 < s \leqslant d_3$ is also adiabatic and contains saturated vapor. To complete the cycle, condenser section $d_3 < s \leqslant L$ is cooled by a constant heat flux $\dot{q}_c$ where L is the loop length.

Assumptions made in the analysis are:

(1) flow velocity and pressure are steady-state, and one-dimensional functions of the flow distance;

(2) fluid in the entire loop is in the saturated condition;

(3) the Poiseuille flow profile is used to evaluate the friction factor in single phase regions;

(4) the homogeneous model is employed for the two-phase zones;

(5) the quality of the vapour in the two-phase zone varies linearly from one section boundary to the other; and

(6) the friction coefficient in the two-phase zone is constant.

Besides, superheat, subcooling and possible entrainment in the two-phase zones are not considered.

Note that vapour quality usually increases (or decreases) monotonically from the inlet section of the evaporator (or condenser) to the exit section. The assumption of a linear distribution of vapour quality

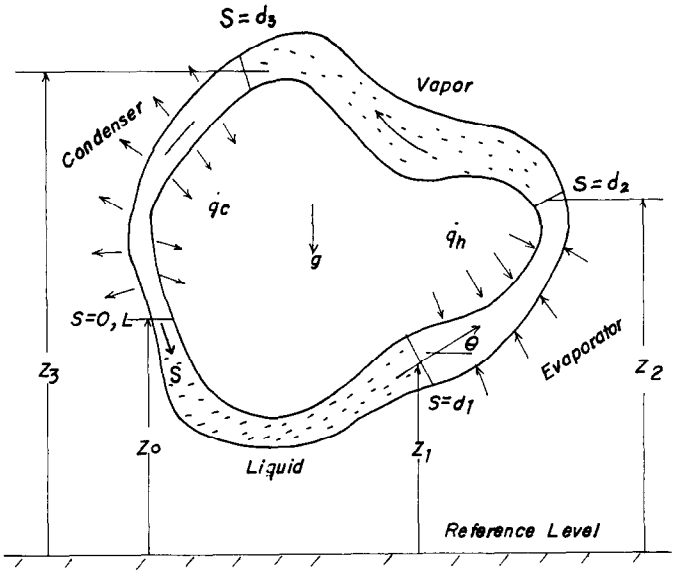

FIG. 2. Schematic and coordinates of a variable-area two-phase natural circulation loop.

in the two-phase segments is therefore frequently employed in the two-phase modelling [13]. It is also noted in ref. [13] that the value of f_{TP} for low-pressure flashing steam–water flow is in the range of 0.0029–0.0033, and is about 0.005 for a high-pressure boiler. In either case, f_{TP} is nearly constant. In this study, a value of $f_{TP} = 0.0031$ is chosen for the analytical development.

Since the homogeneous model is employed in the two-phase zone, the governing equations in the two-phase zone bear the same forms as those in the single phase region [12, 13]. So the one-dimensional, steady-state equations governing the loop flow can be written as

$$\begin{cases} \dot{m} = \rho u A & (1) \\ \dfrac{dp}{ds} = -\dfrac{\tau_w P}{A} - \dfrac{\dot{m}}{A}\dfrac{du}{ds} - \rho g \sin\theta & (2) \\ \dot{Q} = \dot{q}_h l_h = \dot{q}_c l_c = \dot{m} h_{fg}. & (3) \end{cases}$$

Equations (1)–(3) are the continuity, momentum and energy equations, respectively. In equation (2), the pressure drop is due to the viscous, inertia and gravitational losses. In the above equations ρ and τ_w are the mean density and wall friction determined by

$$\rho = \begin{cases} \rho_f, \text{ in the saturated liquid region} \\ \rho_g, \text{ in the saturated vapour region} \\ v^{-1} = [v_f + x v_{fg}]^{-1}, \text{ in the two-phase zone} \end{cases} \quad (4a\text{–}c)$$

$$\tau_w = \begin{cases} B_l u_l, \text{ in the liquid region} \\ B_g u_g, \text{ in the vapour region} \\ f_{TP}\dfrac{\rho u|u|}{2}, \text{ in the two-phase region} \end{cases} \quad (5a\text{–}c)$$

where B is a constant; x and f_{TP} are the quality of vapour and the friction coefficient in the two-phase zone, respectively. For a Poiseuille flow in the single phase region, one can find [14]

$$B_l = \frac{8\pi\mu_l}{P}, \quad B_g = \frac{8\pi\mu_g}{P} \quad (6a,b)$$

where P is the perimeter of the cross-section.

The loop integral of equation (2) requires

$$\int_0^L \frac{dp}{ds}\,ds = 0. \quad (7)$$

Substituting equations (4)–(6) into equation (2) and carrying out the loop integral yields

$$a_1\dot{m}^2 + a\dot{m}|\dot{m}| + b\dot{m} + c = 0 \quad (8)$$

where

$$a_1 = \int_0^L \frac{1}{A}\frac{d}{ds}\left(\frac{1}{\rho A}\right)ds \quad (9a)$$

$$a = 2\pi\int_{d_1}^{d_2} \frac{f_{TP}}{\rho P A^2}\,ds + 2\pi\int_{d_3}^{L} \frac{f_{TP}}{\rho P A^2}\,ds \quad (9b)$$

$$b = \int_0^{d_1} \frac{B_l P}{\rho A^2}\,ds + \int_{d_2}^{d_3} \frac{B_g P}{\rho A^2}\,ds \quad (9c)$$

$$c = \int_0^L \rho g \sin\theta\,ds. \quad (9d)$$

In equation (9d), θ is the angle of flow measured from the horizontal, and the following relation holds:

$$dz = \sin\theta\,ds \quad (10)$$

where z is the vertical height from the datum plane (Fig. 2).

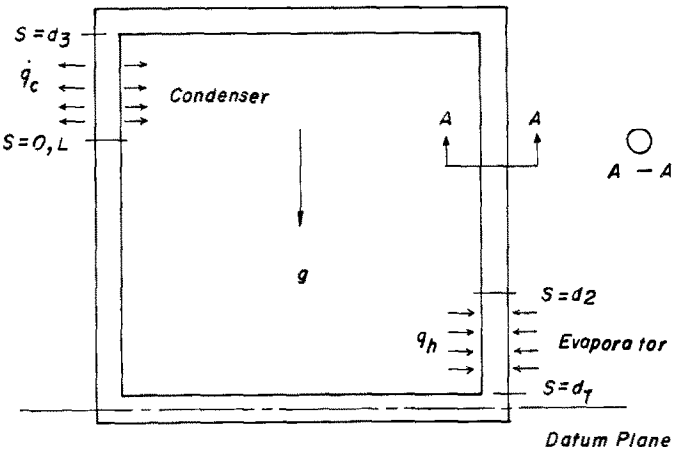

FIG. 3. Physical model and coordinates for a constant-area square loop.

It can be seen from equation (9a) that 'a_1' represents the variation of cross-sectional area; 'a' in equation (9b) represents two-phase friction forces in the heating and cooling sections; 'b' in equation (9c) represents the single phase friction forces in the saturated liquid and vapour zones; and 'c' in equation (9d) is simply the net driving force, or net buoyant force, around the loop due to the density difference between the liquid and vapour phases.

If the loop is of variable area such that 'a_1' in equation (8) is not equal to zero, multiple solutions are obtained. However, for a loop of constant area as considered in the following sections, $a_1 = 0$ and there is only one solution given by

$$\dot{m} = \frac{-b+\sqrt{(b^2-4ac)}}{2a} \tag{11}$$

provided that

$$b^2-4ac \geqslant 0. \tag{12}$$

Note that in the present study, the evaporator is located on the right leg of the loop, so only the positive value of $\dot{m}$ needs to be considered. It can be shown later that the value of 'c' is related to the liquid-level difference between the evaporator and condenser sections. If the evaporator is placed below the condenser as usually done in the system of waste heat recovery, 'c' is always negative. Because values of 'a' and 'b' shown in equations (9b) and (9c) are always positive, so equation (12) can always be satisfied.

It is clear from equations (9a) to (9d) that the functional relation $A(s)$, $\rho(s)$, f_{TP}, B_l and B_g must be known in order to evaluate a, b and c. That is, the loop shape, dimensions and fluid properties must be known in advance. In what follows, analysis will be focused on constant-area, square and toroidal loops as shown in Figs. 3 and 4, respectively.

3. CONSTANT-AREA SQUARE LOOP

The physical model and coordinate system for a square loop is shown in Fig. 3. The central line of the lower horizontal branch is taken to be the datum plane. From equation (4c), $\rho(s)$ is prescribed if $x(s)$, the vapour quality as a function of flow distance, is known. In this study, a linearly varying function is assumed for $x(s)$ according to

$$\begin{aligned} &0 < s \leqslant d_1: && x = 0 \\ &d_1 < s \leqslant d_2: && x = (s-d_1)/l_h \\ &d_2 < s \leqslant d_3: && x = 1 \\ &d_3 < s \leqslant L: && x = (L-s)/l_c. \end{aligned} \tag{13a–d}$$

That is vapour quality is linearly increasing in the evaporator section, and is linearly decreasing in the condenser section. Substituting equations (6a), (6b), (13a) and (13b) into equations (9a)–(9d) and using relation (10) gives

$$a = \frac{2\pi f_{TP}}{PA^2}\left[v_f l_h + \frac{v_{fg}}{2} l_h + v_f l_c + \frac{v_{fg}}{2} l_c\right] \tag{14}$$

$$b = \frac{B_l P v_f}{A^2} d_1 + \frac{B_g P}{A^2}(d_3-d_2)v_g \tag{15}$$

$$c = -\rho_f g \Delta z_l - \frac{g l_h}{v_{fg}} \ln\left[1+\frac{v_{fg}}{v_f}\frac{(z_2-z_1)}{l_h}\right] + \rho_g g \Delta z_g + \frac{g l_c}{v_{fg}} \ln\left[1+\frac{v_{fg}}{v_f}\frac{(z_3-z_0)}{l_c}\right]. \tag{16}$$

In the above

$$l_c = z_3 - z_0, \quad l_h = z_2 - z_1 \tag{17a,b}$$

$$\Delta z_l = z_0 - z_1, \quad \Delta z_g = z_3 - z_2 \tag{18a,b}$$

where l_h and l_c are the heating (evaporator) and cooling (condenser) lengths, respectively; Δz_l the liquid-level difference, and Δz_g the vapour-level difference. Note that in arriving at equation (14) we have used the assumption that f_{TP} is nearly constant in the two-phase zone, and $f_{TP} = 0.0031$ is chosen in the numerical calculations.

Because liquid density is usually much larger than vapour density ($\rho_f \cong 1500\rho_g$ for water as an example),

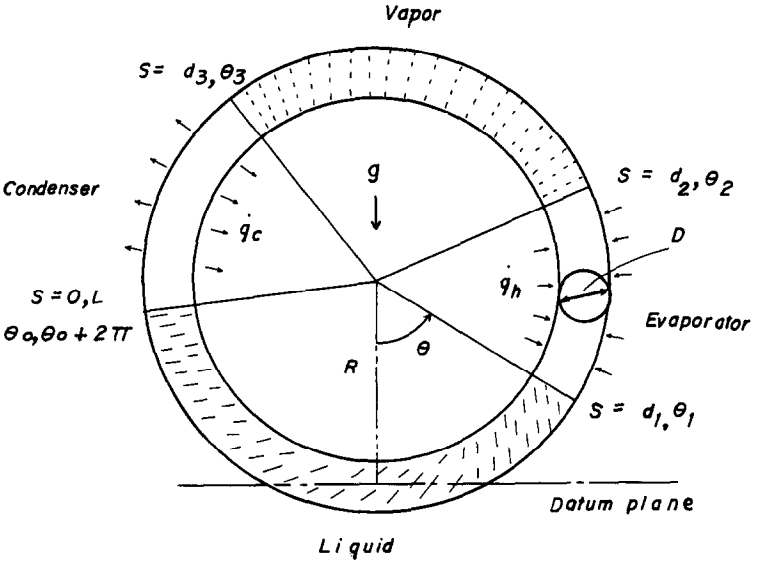

FIG. 4. Physical model and coordinates for a constant-area toroidal loop.

the value of 'c' shown in equation (16) is always negative if the evaporator is placed below the condenser ($\Delta z_l > 0$), unless the condenser length l_c is impractically extremely long. Therefore, the net driving force 'c' is dominated by the liquid-level difference. If the evaporator and condenser are equal in length l, then equation (16) can be simplified as

$$c \cong -\rho_f g \Delta z_l. \tag{19}$$

That is, the net driving force 'c' is mainly contributed by the liquid-level difference Δz_l.

4. CONSTANT-AREA TOROIDAL LOOP

The physical model for a toroidal loop and its coordinate system are shown in Fig. 4. For convenience, the datum plane is taken to be the horizontal line passing through the lowest point of the loop. The following relation holds for a toroidal loop:

$$\mathrm{d}z = R \sin\theta \, \mathrm{d}\theta \tag{20}$$

where $-\pi \leqslant \theta \leqslant \pi$, and θ is measured counterclockwise from the lowest point in the loop (Fig. 4).

As in a square loop, the quality of vapour in the loop is assumed to be a linearly varying function of the flow distance according to

$$0 < s \leqslant d_1: \; x = 0$$

$$d_1 < s \leqslant d_2: \; x = (\theta - \theta_1)/(\theta_2 - \theta_1)$$

$$d_2 < s \leqslant d_3: \; x = 1$$

$$d_3 < s \leqslant L: \; x = (2\pi + \theta_0 - \theta)/(2\pi + \theta_0 - \theta_3). \tag{21a–d}$$

Substituting equations (6a), (6b), (21a) and (21b) into equations (9a)–(9d) and using relation (20) gives

$$a = \frac{2Rf_{TP}}{DA^2}\left[v_f(\theta_2 - \theta_1) + \frac{v_{fg}}{2}(\theta_2 - \theta_1) + v_f(2\pi + \theta_0 - \theta_3) + \frac{v_{fg}}{2}(2\pi + \theta_0 - \theta_3) \right] \tag{22}$$

$$b = \frac{Rv_f B_l P}{A^2}(\theta_1 - \theta_0) + \frac{Rv_g B_g P}{A^2}(\theta_3 - \theta_2) \tag{23}$$

$$c = g\left[-\rho_f \Delta z_l + \int_{\theta_1}^{\theta_2} \frac{R \sin\theta \, \mathrm{d}\theta}{v_f + \dfrac{v_{fg}(\theta - \theta_1)}{(\theta_2 - \theta_1)}} + \rho_g \Delta z_g + \int_{\theta_3}^{2\pi + \theta_0} \frac{R \sin\theta \, \mathrm{d}\theta}{v_f + \dfrac{v_{fg}(2\pi + \theta_0 - \theta)}{(2\pi + \theta_0 - \theta_3)}} \right]. \tag{24}$$

In the above

$$l_c = R(2\pi + \theta_0 - \theta_3), \; l_h = R(\theta_2 - \theta_1) \tag{25a,b}$$

$$\Delta z_l = R(\cos\theta_1 - \cos\theta_0), \quad \Delta z_g = R(\cos\theta_2 - \cos\theta_3). \tag{26a,b}$$

Similarly for a square loop, the value of 'c' is always negative in a practical system, in which the evaporator is placed below the condenser. Note that even if $l_h = l_c = l$, the second and the fourth terms on the right-hand side of equation (24) cannot be cancelled out exactly due to the integral of the sine function. However, the sum of these two terms is very small as compared with the first term. Consequently equation (24) can still be simplified as

$$c \cong -g\rho_f \Delta z_l \tag{27}$$

if $l_h = l_c = l$.

Table 1. Dimensions of square (I) and toroidal (II) loops and properties of saturated water at 1 atm

	P	18.85 cm
I	A	28.26 cm^2
	L	4 m
	θ_0	$-80°$
II	R	0.5 m
	D	4.0 cm
	μ_f	2.831×10^{-4} N s m^{-2}
	μ_g	1.206×10^{-5} N s m^{-2}
	ρ_f	935.31 kg m^{-3}
	v_{fg}	1.6719 m^3 kg^{-1}

Again, the liquid-level difference is the main driving force.

5. RESULTS AND DISCUSSIONS

The above analyses for constant-area square and toroidal loops will be applied to some particular loop dimensions with water–steam as the working fluid. The loop dimensions and fluid properties at 1 atm are listed in Table 1. In all cases, evaporator and condenser are equal in length; that is $l_h = l_c = l$.

Figure 5 presents the functional relations of $\dot{m}$ vs Δz_l for a square loop with l as a parameter. The loop length is 4 m and flow cross-sectional area is 28.26 cm^2. Figure 5 shows that $\dot{m}$ increases with increasing Δz_l, for a fixed l. It can be seen from equation (19) that a larger Δz_l provides a larger buoyant force and, therefore, results in a larger mass flow rate. For a fixed Δz_l, increasing two-phase zone length results in the increase of the two-phase zone frictional force, that is, 'a' in equation (14) increases; but the net buoyant force 'c' in equation (16) remains the same. Also, it will be seen later that the value of 'b' representing frictional forces in single phase regions changes little. Consequently, the mass flow rate decreases with increasing two-phase zone length under a fixed water-level difference.

Figure 6 presents the functional relation of $\dot{m}$ vs $\Delta\theta_h$ $(=\theta_2-\theta_1)$ as the parameter for a toroidal loop at $R = 50$ cm, $A = 12.57$ cm^2, $P = 15.27$ cm, and $\theta_0 = -80°$. Note that since Δz_l and $\Delta\theta_h$ are related to θ_1 and l_h according to equations (25b) and (26a), respectively, so Fig. 6 in fact shows the dependence of $\dot{m}$ on $-\Delta z_l$ with l as the parameter. Similarly as in a square loop, it shows that the mass flow rate increases with decreasing θ_1 (or increasing Δz_l) for a fixed $\Delta\theta_h$ (or two-phase zone length); and it decreases with increasing two-phase zone length under a fixed water-level difference. Because mass flow rate is proportional to the heat input or output according to equation (3), the water-level difference and two-phase zone length, therefore, affect the recovered heat in the same manner.

The individual terms in equation (2) are, respectively, pressure, friction, inertia and buoyancy forces. Once the mass flow rate has been determined, their functional dependencies on the coordinate s can be obtained by integrating them along the flow distance. For example, the pressure $p(s)$ can be determined by

$$p(s) = p(0) - \int_0^s \frac{\tau_w P}{A}\,ds - \int_0^s \frac{\dot{m}}{A}\frac{du}{ds}\,ds - \int_0^s g\sin\theta\,d\theta \tag{28}$$

where $p(0)$ at $s = 0$ has to be prescribed. Consider the case for a toroidal loop with the following dimensions:

$$\theta_1 = 50°, \quad \theta_0 = -80°$$

$$R = 50\text{ cm}, \quad A = 12.57\text{ cm}^2$$

$$\theta_2 - \theta_1 = 2\pi + \theta_0 - \theta_3 = 30°$$

and the corresponding profiles of pressure, buoyancy, inertia and friction forces as functions of coordinate s are shown in Fig. 8. From Fig. 6 it reads

$$\dot{m} = 0.2213\text{ kg s}^{-1}.$$

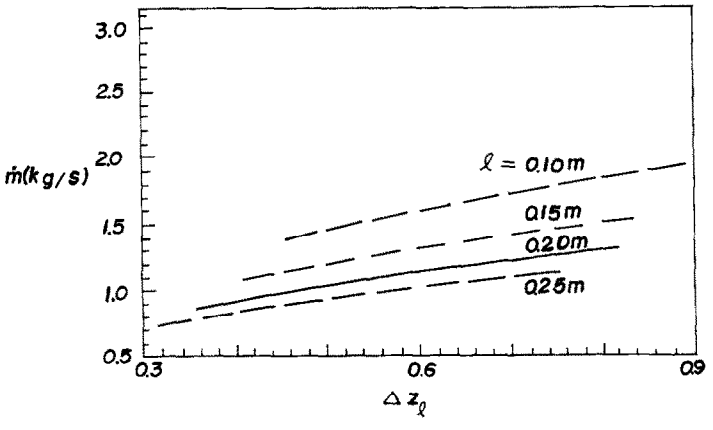

FIG. 5. Mass flow rate as functions of water-level difference and two-phase zone length for a square loop with dimensions given in Table 1.

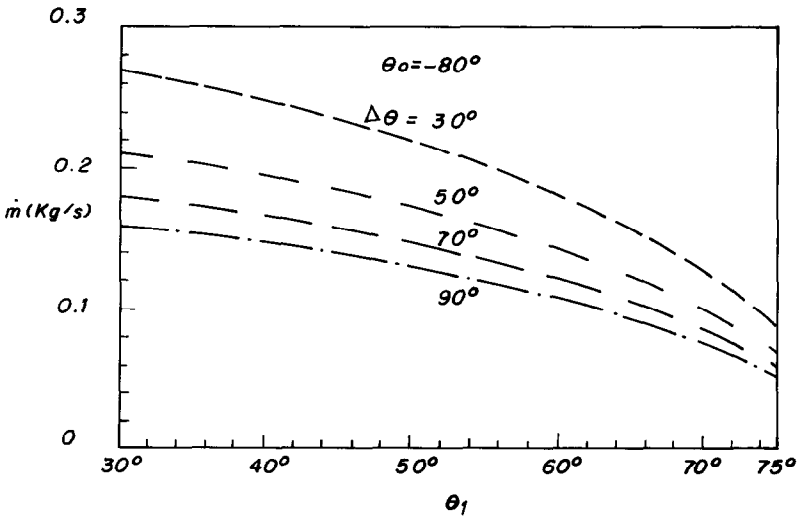

FIG. 6. Mass flow rate as functions of water-level difference and two-phase zone length for a toroidal loop with dimensions given in Table 1.

All forces have been assigned to zero at the origin. Interpretation of the profiles is aided by a diagram of the normalized gravity acceleration function, $\mathbf{g}/g$, given in the lower part of the figure as a function of s. The positive value of $\mathbf{g}/g$ corresponds to the downcoming section of the loop, while the negative value corresponds to the rising section. Coordinates for each boundary of the flow regime, such as $s = d_1$, $d_2, \ldots$, are also indicated in the diagram. Therefore, the single phase liquid region lies in $0 < s \leqslant d_1$; the evaporator section lies in $d_1 < s \leqslant d_2$, and so on.

It can be seen from Fig. 8 that pressure and buoyancy forces are dominant in the liquid region, where friction and inertia forces are negligible. The inertia force starts increasing once the flow enters the evaporator section and remains nearly constant in the single phase vapour zones, and then decreases in the condenser section. Pressure and inertia forces are dominant in the evaporator and single phase vapour zones. The frictional force in the vapour and two-phase zones is small, but it is of comparable order to the buoyant force. The momentum balance requires that the summation of the individual forces vanishes at each location of the loop. Also, the loop or cycle integrals for the pressure and inertial forces go to zero, but are non-zero and opposite in sign and equal in magnitude for the buoyant and frictional forces. It is this net buoyant force that drives fluid circulating around the loop and balances the frictional force.

If flow cross-sectional area is decreased but other loop dimensions are kept the same, the individual force contributions are shown in Fig. 9 for a toroidal

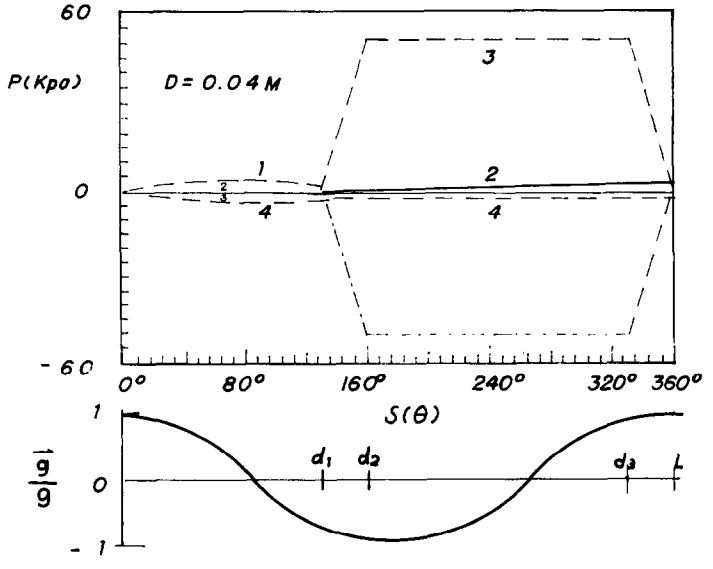

FIG. 7. Mass flow rate as functions of water-level difference and flow cross-sectional area for a toroidal loop with dimensions given in Table 1 and $\Delta\theta = 30°$.

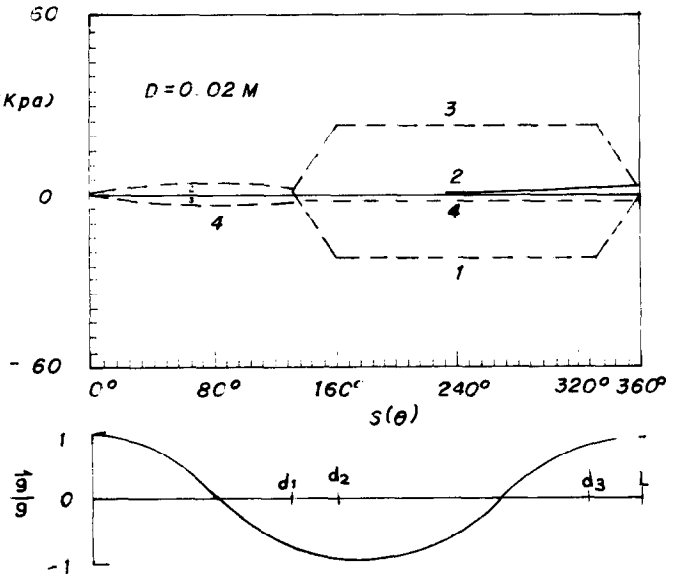

FIG. 8. Distributions of individual forces around a toroidal loop with $A = 12.57$ cm^2: 1, pressure; 2, friction; 3, inertia; 4, buoyancy force.

loop with $A = 3.14$ cm^2. Comparison with Figs. 8 and 9 shows that pressure and inertia forces decrease significantly when the pipe diameter reduces from 4 to 2 cm, but buoyant and frictional forces change little. Since mass flow rate is proportional to the inertia force, it decreases with decreasing flow cross-sectional area accordingly. A similar effect also holds for the recovered heat.

6. CONCLUSIONS

A one-dimensional steady-state analysis of a variable-area, two-phase natural convection loop based on a homogeneous two-phase model is presented. The quality of vapour in the two-phase zone is assumed to be a linearly varying function of the flow distance. Effects of two-phase zone lengths, liquid-level difference and flow cross-sectional area on the mass flow rate and recovered heat are examined for constant-area, square, and toroidal loops with water–steam as the working fluid. The conclusions given below can be drawn from this study.

(1) Mass flow rate or recovered heat increases with increasing water-level difference under a fixed two-phase zone length due to the increasing net driving force.

(2) Mass flow rate or recovered heat decreases with

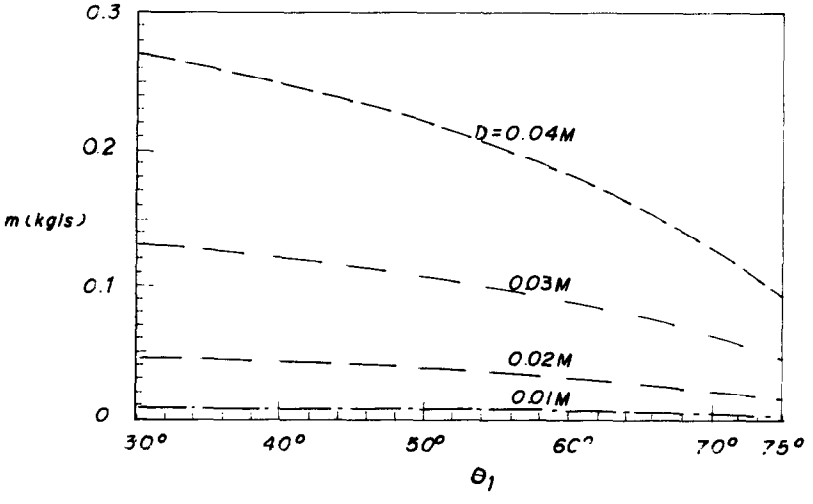

FIG. 9. Distributions of individual forces around a toroidal loop with $A = 3.14$ cm^2; see Fig. 8 for the symbols.

increasing two-phase zone length under a fixed water-level difference primarily due to the increase of two-phase frictional force.

(3) Mass flow rate or recovered heat decreases with decreasing flow cross-sectional area for a fixed loop diameter or loop length primarily due to the decrease of inertia force.

(4) Because recovered heat is also proportional to the latent heat of evaporation, a fluid with a large value of h_{fg} is desirable for the purpose of waste heat recovery.

REFERENCES

1. H. R. McKee, Thermosyphon reboilers—a review, *Ind. Engng Chem.* **62,** 76–82 (1970).
2. N. V. L. A. Sarma, P. J. Reddy and P. S. Murti, A computer design method for vertical thermosyphon reboilers, *Ind. Engng Process Des. Dev.* **12,** 278–290 (1973).
3. D. B. Bandy and S. G. Bankoff, Optimal design of a natural-circulation boiling-water channel. In *Progress in Heat and Mass Transfer* (Edited by U. Grigull and E. Hahne), Vol. 1, pp. 425–471. Pergamon Press, New York (1969).
4. Y. Y. Hsu, Two-phase flow problems in pressurized-water reactors. In *Thermohydraulics of Two-phase Systems for Industrial Design and Nuclear Engineering* (Edited by J. M. Delhaye, M. Giot and M. L. Riethmuller), pp. 1–10. Hemisphere, Washington, DC (1981).
5. J. A. Block, Emergency cooling water delivery to the core inlet of PWRs during LOCA, Creare TM-529 (1976).
6. R. T. Fernandez, J. P. Sursock and R. L. Kiang, Reflux boiling heat removal in a sealed TMI-2 system test facility, ANS/ENS Thermal Reactor Safety Meeting, Knoxville, Tennessee, April (1980).
7. D. Japikse, Advances in thermosyphon technology. In *Advances in Heat Transfer*, Vol. 97, pp. 367–386 (1981).
8. Y. Zvirin, A review of natural circulation loops in pressurized water reactors and other systems, *Nucl. Engng Des.* **67,** 203–225 (1981).
9. A. Mertol and R. Greif, A review of natural circulation loops. In *Natural Convection: Fundamentals and Applications* (Edited by S. Kakac, W. Aung and R. Viskanta), pp. 1033–1071. Hemisphere, Washington, DC (1985).
10. Technical Presentation Document of Blast Furnace Hot Stove Waste Heat Recovery System (Hitachi Separate Type Heat Pipe) for China Steel Corporation, Hitachi Ltd., Babcock–Hitachi K. K., September (1985).
11. E. Ramos, M. Sen and C. Trevino, A steady-state analysis for variable area one- and two-phase thermosyphon loops, *Int. J. Heat Mass Transfer* **28,** 1711–1719 (1985).
12. G. B. Wallis, *One-dimensional Two-phase Flow*, pp. 17–35. McGraw-Hill, New York (1969).
13. J. G. Collier, *Convective Boiling and Condensation*, pp. 30–35. McGraw-Hill, New York (1972).
14. F. M. White, *Fluid Mechanics*, pp. 324–325. McGraw-Hill, New York (1979).

ANALYSE D'UNE BOUCLE DE CIRCULATION PERMANENTE NATURELLE DIPHASIQUE

Résumé—On considère des boucles de circulation permanente naturelle, par exemple des thermosiphons, pour lesquelles la différence de densité du fluide entre ses phases liquide et vapeur est la cause motrice. Les équations unidirectionnelles sont d'abord formulées pour un circuit à section variable, diphasique, à partir du modèle homogène. De plus, la qualité de la vapeur dans la zone diphasique est supposée être une fonction linéaire de la distance longitudinale. Le modèle est ensuite appliqué à des boucles à section constante, carrée et toroïdale, avec l'eau comme fluide actif. Pour une taille donnée, l'effet de la position relative entre l'évaporateur et le condenseur peut être évalué en fonction de la différence de niveau d'eau liquide entre eux. Les résultats montrent que le débit-masse et la chaleur récupérée augmentent quand cette différence de niveau croît, pour une longueur de zone diphasique fixée, à cause de l'accroissement des forces de flottement, tandis qu'ils diminuent quant la longueur de zone diphasique augmente, pour une différence de niveau d'eau fixée, à cause de l'accroissement de la force de frottement en diphasique. Dans un projet de récupération de chaleur perdue, un fluide à grande chaleur latente de changement d'état est souhaitable puisqu'il est capable d'accepter plus de chaleur pour un débit-masse donné.

THEORETISCHE UNTERSUCHUNG DES STATIONÄREN VERHALTENS EINES ZWEIPHASIGEN NATURUMLAUFSYSTEMS

Zusammenfassung—Diese Arbeit befaßt sich mit dem stationären Verhalten von Zweiphasen-Naturumlauf-Systemen, z. B. Thermosyphons, in welchen der Dichteunterschied zwischen Flüssigkeit und Dampfphase als Antriebskraft dient. Es werden die eindimensionalen Strömungsgleichungen, beruhend auf dem homogenen Modell, für einen Zweiphasen-Kreislauf mit veränderbarem Querschnitt formuliert. Ergänzend wird angenommen, daß der Massendampfgehalt im Zweiphasengebiet linear vom Strömungsweg abhängt. Das Modell wird dann auf einen quadratischen Kreislauf und einen Torus mit konstantem Querschnitt für das Arbeitsmittel Wasser-Dampf angewandt. Bei gegebener Größe und Form des Kreislaufs kann der Einfluß der relativen Lage von Verdampfer und Kondensator mit Hilfe der Wasserspiegeldifferenz zwischen ihnen ausgedrückt werden. Die Ergebnisse zeigen, daß Massenstrom und transportierter Wärmestrom bei wachsender Wasserspiegeldifferenz und unter konstant gehaltener Länge des Zweiphasengebiets infolge der zunehmenden Auftriebskräfte größer werden; sie werden dagegen bei zunehmender Länge des Zweiphasengebiets und unter konstant gehaltener Wasserspiegeldifferenz infolge des zunehmenden Zweiphasen-Strömungswiderstandes kleiner. Bei gegebenem Kreislaufdurchmesser oder Kreislauflänge verringern sich Massenstrom und Wärmestrom bei verringertem Strömungsquerschnitt unter konstant gehaltener Wasserspiegeldifferenz und Länge des Zweiphasengebiets.

АНАЛИЗ СТАЦИОНАРНОГО РЕЖИМА ДВУХФАЗНОГО КОНТУРА С ЕСТЕСТВЕННОЙ ЦИРКУЛЯЦИЕЙ

Аннотация—Рассматривается стационарный режим двухфазных контуров с естественной циркуляцией, т.е. термосифонов, в которых движущей силой является разность между плотностями жидкой и паровой фаз. Впервые сформулированы одномерные определяющие уравнения для таких контуров переменного сечения. Кроме того принимается, что свойства пара в двухфазной зоне линейно изменяются от пути течения. Эта модель затем применяется к квадратным и тороидальным контурам постоянного сечения, рабочей жидкосты в которых явдяется водопаровая смесь. Для контура заданных размеров и формы влияние относительного положения между испарителем и конденсатором может быть оценено через разность уровней воды в них. Результаты показывают, что массовый расход в контуре и возвращенное тепло возрастают с увеличением разности в уровнях воды при фиксированной длине двухфазной зоны в результате роста подъемной силы. В то самое время они уменьшаются с увеличением длины двухфазной зоны при фиксированной разности уровней воды в результате роста силы трения в двухфазном потоке. При заданных диаметре или длине контура массовый расход и возвращенная теплота с уменьшением площади поперечного сечения потока при фиксированных разности уровней воды и длине двухфазной зоны первоначально уменьшаются из-за уменьшения сил инерции по контуру. Для восстановления отработанного тепла желательно использовать жидкость с большей скрытой теплотой испарения, поскольку в ней выделяется больше тепла при заданном массовом расходе.